Numerical demonstration of three-dimensional terahertz metamaterials based on the causality principle

Saeid Jamilan†, Javad Nourinia, and Mohammad Naghi Azarmanesh

Department of Electrical Engineering, Urmia University, Urmia, Iran

(Received 8 July 2013; revised manuscript received 16 August 2013; published online 20 December 2013)

A parameter retrieval algorithm based on the causality principle and Kramers–Kronig (KK) relations is employed to calculate the effective parameters of three-dimensional (3D) metamaterials. Using KK relations, the branch selecting problem, which is the challenge of effective parameter retrieval method, can be removed. To reveal the validity of the proposed algorithm, the constitutive refractive index of a homogeneous polymide cube is extracted. The result is in excellent agreement with the intrinsic refractive index of the polymide. Finally, the two terahertz metamaterials with 3D structures are designed and their effective parameters are then retrieved using the proposed algorithm. Numerical simulations are performed using the full-wave electromagnetic solver, CST Microwave Studio.

Keywords: metamaterial, three-dimensional, causality principle, Kramers–Kronig relations

PACS: 78.67.Pt, 78.20.Ci, 87.50.U–

DOI: 10.1088/1674-1056/23/2/027804

1. Introduction

Since the first experimental demonstration of negative refraction by Smith *et al.*,[1] metamaterials with negative permittivity and permeability that cannot be found from among naturally occurring materials have attracted considerable attention. Metamaterials have found enormous applications in cloaks,[2] perfect lenses,[3] and absorbers.[4–6] In 1996, Pendry *et al.*[7] introduced the first artificial material, which consisted of thin wires and had an effective permittivity with a negative real part in the lower frequency band. Pendry *et al.*[8] also presented a material with negative permittivity composed of two-dimensional (2D) thin wires in 1998.

Artificial materials made of split ring resonators (SRRs) having negative permeability were first introduced by Pendry *et al.*[9] in 1999. A combination of thin wires and SRRs showed a negative refraction index and was presented by Smith *et al.*[1] in 2000. In addition, other various resonator structures such as spiral resonators[10] and S-shaped resonators[11] have been designed to have negative values for their refractive indices.

Most early developments in metamaterials operated in the microwave regime due to the simplicity in fabrication and measurement. Metamaterials are of particular interest in the terahertz regime, where most natural materials exhibit only weak electric and magnetic responses. The introduction of terahertz metamaterials provides the possibility to construct novel terahertz devices for practical applications such as modulators,[12] absorbers,[13] and filters.[14] While the physical properties can already be demonstrated in 2D metamaterials, practical applications require 3D structures.[15] In recent years, various metamaterial structures which operate over terahertz and optical frequencies have been designed and fabricated using fabrication techniques such as membrane-projection lithography, focused ion beam lithography, electron beam lithography, direct laser writing, atomic layer deposition and multilayer electroplating. Some of these techniques have been used for 3D structuring.[16–20]

In this paper, we present the design and characterization of two 3D metamaterial structures which operate over terahertz frequencies. An algorithm based on the causality principle and Kramers–Kronig (KK) relations is employed for the accurate extraction of effective parameters of the proposed 3D metamaterial structures. Proposed 3D metamaterials each have a cubic configuration with micrometer dimensions. Verification of the proposed method is presented by retrieving the constitutive refractive index of a homogeneous polymide cube.

2. Retrieving the effective parameters using the causality principle

Extracting the effective parameters of the metamaterials is a critical concept in metamaterial design and can be achieved by several approaches, of which the *S*-parameter method is the most prevalent.[21,22] In fact, the idea is to model the metamaterial as a homogenous slab, and to calculate the effective parameters of the homogenous slab using *S*-parameters based on the effective medium theory. One way to generate the *S*-paramaters of a metamaterial slab is to model it with an FDTD solver such as CST microwave studio or Ansoft HFSS using periodic boundary condition (PBC). The boundary surface perpendicular to the incident $\boldsymbol{E}$ field is defined as a perfect electric conductor (PEC) surface, while the surface perpendicular to the incident $\boldsymbol{H}$ field is defined as a perfect magnetic conductor (PMC) surface. Finally, the surface perpendic-

†Corresponding author. E-mail: saeid.jamilan@gmail.com

© 2014 Chinese Physical Society and IOP Publishing Ltd

ular to propagation vector ($\boldsymbol{k}$) is defined as open port. When the S-parameters of the metamaterial slab are obtained by an FDTD solver, we can determine the effective wave impedance z, refractive index n, effective electric permittivity ε, and effective magnetic permeability μ of this metamaterial by the S-parameter method which can be described as follows:[21,22]

$$z = \pm\sqrt{\frac{(1+S_{11})^2 - S_{21}^2}{(1-S_{11})^2 - S_{21}^2}}, \tag{1}$$

$$\mathrm{e}^{\mathrm{i}nk_0d} = \frac{S_{21}}{1 - S_{11}\dfrac{z-1}{z+1}}, \tag{2}$$

$$\varepsilon = \frac{n}{z}, \quad \mu = nz, \tag{3}$$

where k_0 is the wave number of the incident wave and d is the effective thickness of the unit cell of metamaterial. The ambiguity on the sign of Eq. (1) is prevented if account is held, owing to the fact that the real part of the impedance is positive if it is a passive medium, and the imaginary part of the refractive index is positive to ensure that the incident wave amplitude decreases inside the structure. The complex refractive index can be calculated from

$$n = \frac{1}{k_0 d}\{\mathrm{Im}[\ln(\mathrm{e}^{\mathrm{i}nk_0d})] + 2m\pi - \mathrm{i}\mathrm{Re}[\ln(\mathrm{e}^{\mathrm{i}nk_0d})]\}, \tag{4}$$

where m is an integer related to the branch index of n and "Re" and "Im" denote the real and imaginary parts, respectively. Since complex logarithmic function is a multi-branch one, refractive index n cannot be uniquely determined using Eq. (4). Assuming that $n = \mathrm{Re}(n) + \mathrm{i}\mathrm{Im}(n)$, we can write

$$\mathrm{Im}(n) = \frac{-\mathrm{Re}[\ln(\mathrm{e}^{\mathrm{i}nk_0d})]}{k_0 d}, \tag{5}$$

$$\mathrm{Re}(n) = \frac{\mathrm{Im}[\ln(\mathrm{e}^{\mathrm{i}nk_0d})]}{k_0 d} + \frac{2m\pi}{k_0 d} = n_0 + \frac{2m\pi}{k_0 d}, \tag{6}$$

where n_0 is the real part of refractive index corresponding to the principal branch of the logarithmic function with $m = 0$. The integer number m in Eq. (6) is referred as a branching problem, which affects only the real part of the refractive index. Recently an improved method introduced in Ref. [23] and developed in Ref. [24] based on the causality principle and KK relations for extracting effective parameters of metamaterials. The KK dispersion rules connect the real and imaginary parts of the material parameters and also lead to important integral relations, so-called sum rules, for electromagnetic parameters of medium.[25] In this method, the branch selecting is performed according to the approximation solution of the real part of the refractive index obtained from KK relations. The imaginary part of refractive index can be unambiguously determined using Eq. (5). Considering this fact, KK relations which connect the real and imaginary parts of the material parameters based on the causality principle are used for solving the branch selecting problem in Eq. (6). This method was demonstrated in Ref. [24] and the proposed method is then employed for extracting the parameters of 2D metamaterial structures with different effective thickness values. In this paper, we perform an algorithm based on the same approach to retrieving the accurate parameters of the 3D metamaterial structure while the procedure of the algorithm is explained with detailed demonstrations. The KK relations are given by

$$\mathrm{Re}\{a(\omega)\} = \mathrm{Re}\{a(\infty)\} + \frac{2}{\pi}\mathrm{PV}\int_0^\infty \frac{u\,\mathrm{Im}\{a(u)\}}{u^2 - \omega^2}\,\mathrm{d}u, \tag{7}$$

$$\mathrm{Im}\{a(\omega)\} = -\frac{2\omega}{\pi}\mathrm{PV}\int_0^\infty \frac{\mathrm{Re}\{a(u)\} - \mathrm{Re}\{a(\infty)\}}{u^2 - \omega^2}\,\mathrm{d}u, \tag{8}$$

where PV refers to the principal value of the integral, and $a(\omega)$ can be either $\varepsilon(\omega)$, $\mu(\omega)$, or $n(\omega)$ in a metamaterial slab. Substituting $n(\omega)$ into Eq. (7), we can write

$$n^{\mathrm{KK}}(\omega) = 1 + \frac{2}{\pi}\mathrm{PV}\int_0^\infty \frac{u\,\mathrm{Im}\{n(u)\}}{u^2 - \omega^2}\,\mathrm{d}u. \tag{9}$$

Notice that due to the unknown exact value of $\mathrm{Re}\{n(\omega = \infty)\}$, it is assumed that $n(\infty) = 1$. As demonstrated in Refs. [26] and [27], it can be assumed that for very high driving frequency, the frequency will be much higher than any binding frequency of the electrons in the medium, and so the electrons will behave as though they are free. The equation of motion of an electron can be expressed as

$$m_{\mathrm{e}}\ddot{x} = e\boldsymbol{E} = e\boldsymbol{E}_\omega\,\mathrm{e}^{-\mathrm{i}\omega t}, \tag{10}$$

where $\boldsymbol{E}$ is the incident field, m_{e} is the electron mass, and e is the elementary charge. Considering $\boldsymbol{x} = \boldsymbol{x}_\omega\,\mathrm{e}^{-\mathrm{i}\omega t}$ and substituting it into the equation of motion, it can be found that $\boldsymbol{x} = -(e/m_{\mathrm{e}}\omega^2)\boldsymbol{E}$. The polarization of the medium is given by

$$\boldsymbol{P} = \chi(\omega)\boldsymbol{E} = Ne\boldsymbol{x} = -\frac{Ne^2}{m_{\mathrm{e}}\omega^2}\boldsymbol{E}, \tag{11}$$

where N is the number density of the electrons and $\chi(\omega) = (n^2(\omega) - 1)/4\pi$ is the electric susceptibility. By comparing the result of Eq. (11) with the relation of electric susceptibility, we conclude that

$$\chi(\omega) = \frac{1}{4\pi}(n^2(\omega) - 1) \approx -\frac{Ne^2}{m_{\mathrm{e}}\omega^2} \quad (\omega \to \infty). \tag{12}$$

Hence, $n(\omega) \to 1$ as $\omega \to \infty$ from the physical considerations. Equation (9) is an approximate relation determining the general behavior of the KK solution properly. Equation (9), connecting the unambiguous imaginary part of n to its ambiguous real part, can be used for solving the branch selecting problem of Eq. (6). However, in simulations and experiments, S-parameters are measured in the limited frequency ranges, and so the integrations of Eq. (9) should be truncated. For accuracy, the range of the integration should be as large as possible. On the other hand, if the frequency becomes too large, we may

reach a point where the concept of effective medium parameters is not meaningful since the guided wavelengths are on the order of the dimensions of the metamaterial unit cell. Therefore, the upper limit of integration should be truncated at a frequency at which effective medium definition is valid. Therefore, the KK relations yield only an approximate real part of refractive index. To determine an exact value of m, the real part of n with $m = 0$ (principal branch) should be considered according to Eq. (6) and compared with approximate value of real part of refractive index n^{KK} calculated by Eq. (9) using a numerical integration method such as the trapezoid rule. Thus, the value m can be obtained such that the result of Eq. (6) is the closest to the KK approximation of refractive index n^{KK}. Therefore, the branch number m can be expressed as[24]

$$m = \mathrm{Round}\left((n^{\mathrm{KK}} - n_0)\frac{k_0 d}{2\pi}\right), \tag{13}$$

where the function Round ( ) rounds towards the nearest integer. Finally, the branch number m is substituted into Eq. (6), and the proper value of thr real part of the refractive index $\mathrm{Re}(n)$ is calculated. It should be noted that, generally, $\mathrm{Re}(n)$ may be continuous or discontinuous. If the discontinuity perseveres even when the frequency range of the simulation is increased, this indicates that the effective medium theory has reached a limited range. As demonstrated in Ref. [28], the value of m can determine how many wavelengths are inside the slab. If the wavelength in air is λ, then the wavelength in the slab is $\lambda/\mathrm{Re}(n)$. For given frequencies, the thicker slab (compared to the wavelength) corresponds to the higher values of m or, for a given slab, the lower frequency corresponds to the smaller m. In the very low frequency, the wavelength is very large, and the given slab cannot hold one full wavelength, and thus m is usually zero.

3. Verifying the algorithm

In this section, to validate the method, the refractive index of a homogeneous polymide cube is retrieved. The intrinsic parameters of polymide are $\varepsilon = 3.5$, $\mu = 1$, and $n = \sqrt{\varepsilon \times \mu} \approx 1.87$. The geometrical dimensions of the polymide cube are 100 μm × 100 μm × 100 μm. We run the CST Microwave Studio simulations using periodic boundary condition (PBC) to extract the S-parameters of the proposed polymide cube. The effective parameters extraction algorithm is then employed to calculate the refractive index using KK relations. In the next step, we compare the extracted refractive index with the intrinsic refractive index of the polymide. The purpose of this comparison is to reveal the applicability and accuracy of the employed algorithm. The results of the extracted parameters using MATLAB are shown in Figs. 1(a) and 1(b).

The principle branch of refractive index n_0 has a discontinuity at nearly 0.82 THz, which can be seen in Fig. 1(a). We can conclude that the thickness of the proposed polymide cube is comparable to the wavelength of the incident wave. As indicated in Fig. 1(a), no discontinuity is seen in the n^{KK}, so considering the results from the KK relations and properly choosing the value of m, the discontinuity of the real part of the refractive index is removed and the nearest solution to the KK relations is achieved. Figure 1(b) shows the branch number m as a function of frequency. As shown, the branch number m can equal 0 and 1, resulting in the physically correct refractive index. The calculated refractive index using the demonstrated algorithm is independent of the cube thickness (comparable to the wavelength) and equal to intrinsic refractive index of the polymide, which can be seen from Fig. 1(a). Therefore, it can be concluded that the proposed algorithm is correct.

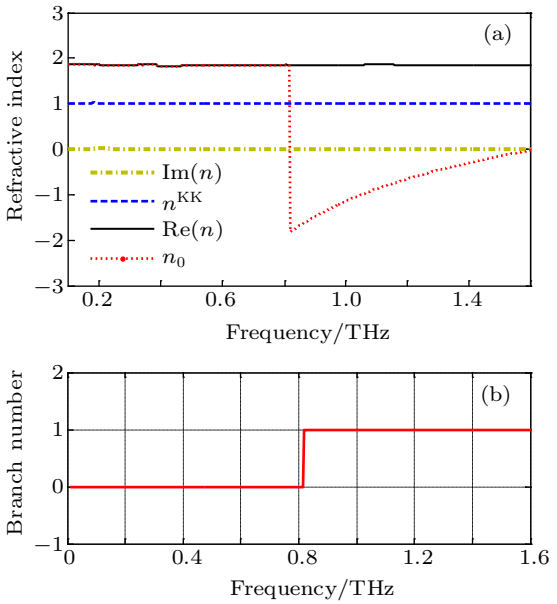


Fig. 1. (color online) Plots of (a) retrieved real and imaginary part of refractive index, KK approximation of refractive index n^{KK}, principal branch of refractive index n_0 of the proposed polymide cube, and (b) branch number m versus frequency.

4. First 3D metamaterial structure

The geometry of the unit cell of the first proposed 3D metamaterial is described in Fig. 2 showing its design parameters and incident EM wave direction. The dielectric substrate of the proposed 3D metamaterial is polymide ($\varepsilon_r = 3.5$ and $\tan\delta = 0.0027$) with a cubic configuration. As shown in Fig. 2, four SRRs are printed on the inner faces of the unit cell and one metal rod placed in the middle of the unit cell. In this 3D metamaterial structure, the role of the SRRs is to provide the negative magnetic permeability, while the role of the rod is to produce the negative electric permittivity. Each of the metallic parts is made of gold with a constant electric conductivity of 4.1×10^7 S/m. The thickness of each of the gold SRRs is 0.2 μm. The numerical simulations for one unit cell are done with CST Microwave Studio with periodic boundary condition. Simulation results of S-parameters are plotted in Fig. 3. We use the demonstrated retrieval algorithm to extract the effective parameters of the proposed 3D metamaterial

structure. Calculated effective impedance, the real and imaginary parts of retrieved refractive index, KK approximation of refractive index n^{KK}, principal branch of refractive index n_0, and integer number m are shown in Figs. 4–6.

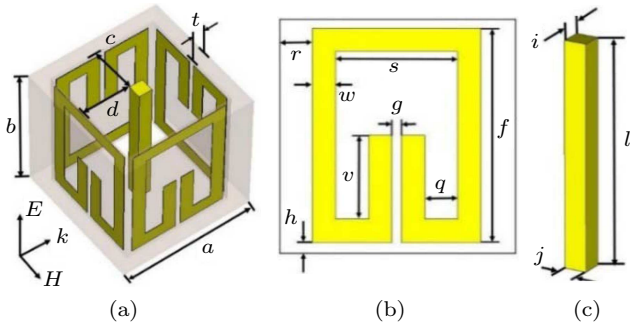


Fig. 2. (color online) (a) Perspective view of unit cell of first proposed 3D metamaterial structure with indicated incident EM wave direction; (b) front view of the unit cell; (c) design parameters of the gold rod. The geometric parameters are as follows: $a = b = 50$ μm, $d = c = 17.5$ μm, $t = 5$ μm, $f = 46$ μm, $r = 7$ μm, $h = 2$ μm, $w = 5$ μm, $s = 26$ μm, $v = 18$ μm, $q = 7$ μm, $g = 2$ μm, $i = j = 5$ μm, and $l = 50$ μm.

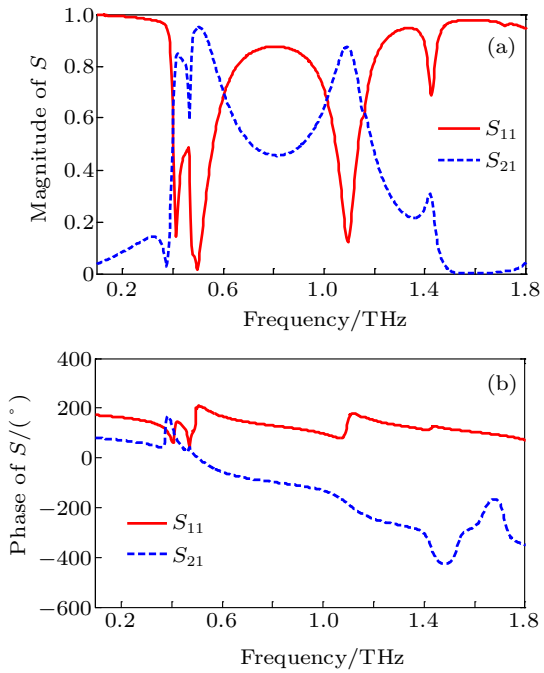


Fig. 3. (color online) (a) Magnitudes and (b) phases versus frequency of the simulated S-parameters for one unit cell of the frist proposed 3D metamaterial.

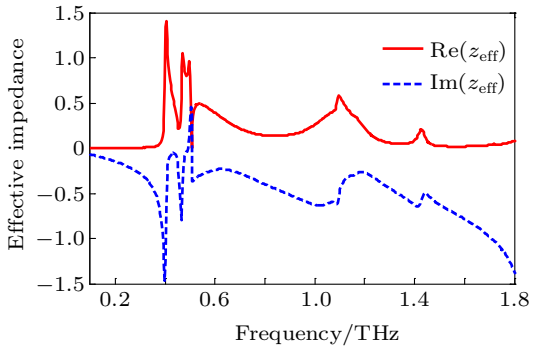


Fig. 4. (color online) Effective impedances versus frequency of the first proposed 3D metamaterial.

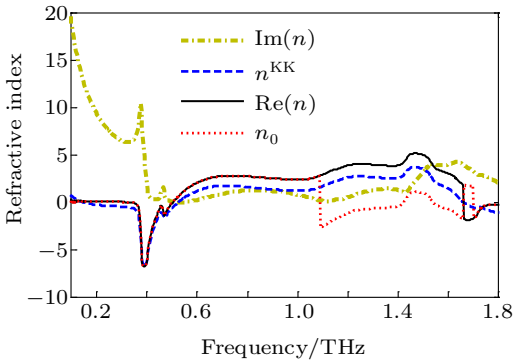


Fig. 5. (color online) Plots of retrieved real and imaginary parts of refractive index, KK approximation of refractive index n^{KK}, and principal branch of refractive index n_0 versus frequency of the first proposed 3D metamaterial.

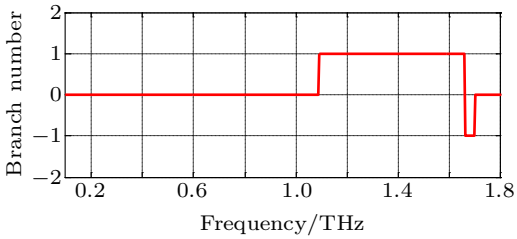


Fig. 6. (color online) Branch number m versus frequency of first proposed 3D metamaterial.

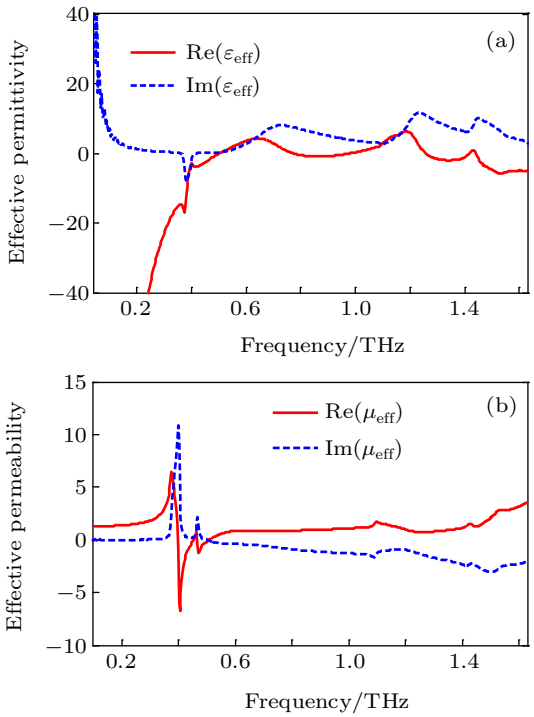


Fig. 7. (color online) Variations of (a) retrieved effective electric permittivity and (b) effective magnetic permeability of the first proposed 3D metamaterial with frequency.

These results show that the principal branch of refractive index is discontinuous at nearly 1.1 THz. The proper integer number m is determined by comparing the curves of KK approximation of refractive index n^{KK} and principal branch of refractive index n_0. By setting proper m, the accurate value of the real part of refractive index is achieved. The discontinuity

of the real part of refractive index at nearly 1.63 THz indicates that the limit of the effective medium theory has been reached and the proposed 3D metamaterial structure can no longer be considered as a homogenous medium. At the discontinuity point at nearly 1.63 THz, the real part of refractive index is $n = 1.84$ and the wavelength in medium can be calculated to be $\lambda \approx 100$ μm. The effective thickness is $a = 50$ μm, which is comparable to the wavelength in medium, $a/\lambda = 0.5$. Therefore, we explain this discontinuity as an upper limit of the effective medium theory. Effective electric permittivity and effective magnetic permeability of this 3D metamaterial structure are presented in Fig. 7.

5. Second 3D metamaterial structure

The geometry of the second proposed 3D metamaterial is shown in Fig. 8, showing its design parameters and incident EM wave direction. The second proposed 3D metamaterial structure is comprised of symmetrical-ring resonators[29] printed on the inner faces of cubic polymide substrate ($\varepsilon_r = 3.5$ and $\tan\delta = 0.0027$) and a symmetrical 3D array of four metal rods in the middle of the structure. In this 3D metamaterial, the symmetrical-ring resonator is to provide the negative magnetic permeability, while the metal rods are to produce the negative electric permittivity. Each of the metallic parts is made of gold with a constant electric conductivity of 4.1×10^7 S/m. The thickness of each of the symmetrical-ring resonators is 0.2 μm. Numerical simulations for one unit cell are performed using CST Microwave Studio, and the extracted S-parameters are plotted in Fig. 9. The results of the retrieved effective impedance, real and imaginary parts of refractive index, KK approximation of refractive index n^{KK}, principal branch of refractive index n_0, and integer number m are presented in Figs. 10, 11, and 12.

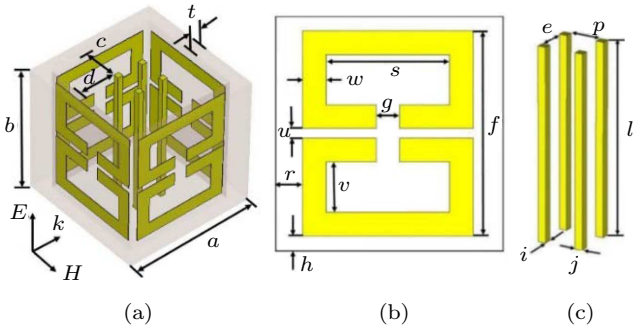


Fig. 8. (color online) (a) Perspective view of unit cell of the second proposed 3D metamaterial structure with indicated incident EM wave direction; (b) front view of the unit cell; (c) design parameters of the gold rods. The geometric parameters are as follows: $a = b = 50$ μm, $t = 5$ μm, $d = 14$ μm, $c = 14$ μm, $f = 43$ μm, $r = 7$ μm, $h = 3.5$ μm, $g = 5$ μm, $u = 2$ μm, $w = 5$ μm, $s = 26$ μm, $v = 10.5$ μm, $i = j = 2$ μm, $l = 50$ μm, and $e = p = 8$ μm.

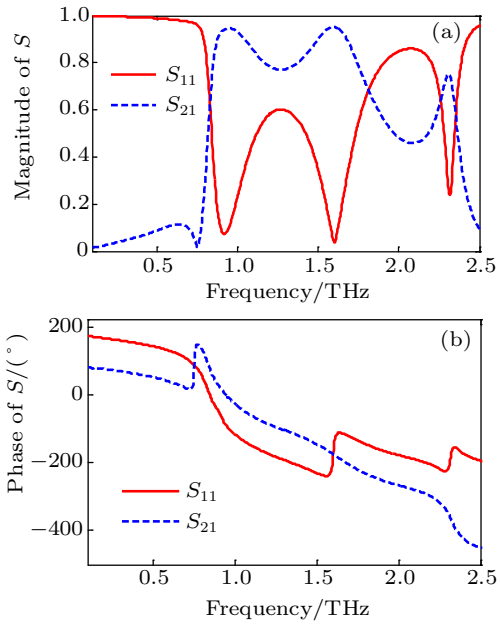


Fig. 9. (color online) Variations of (a) magnitude and (b) phase of the simulated S-parameters with frequency for one unit cell of the second proposed 3D metamaterial.

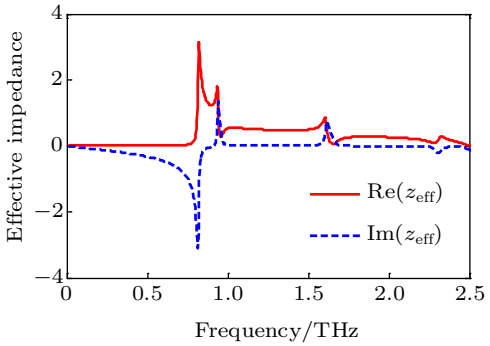


Fig. 10. (color online) Effective impedances versus frequency of the second proposed 3D metamaterial.

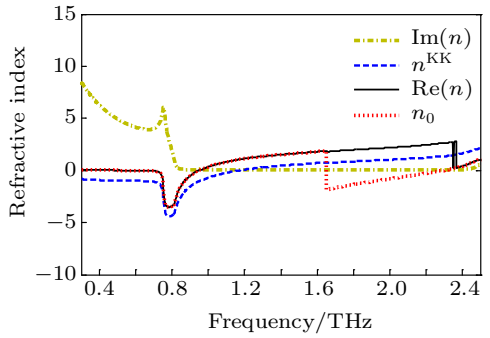


Fig. 11. (color online) Variations of retrieved real and imaginary parts of refractive index, KK approximation of refractive index n^{KK}, and principal branch of refractive index n_0 with frequency of the second proposed 3D metamaterial.

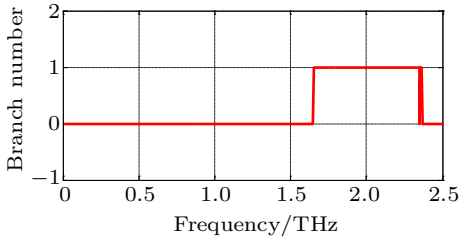


Fig. 12. (color online) Branch number m versus frequency of the second proposed 3D metamaterial.

These results show that principal branch of refractive index is discontinuous at nearly 1.65 THz. By setting proper m, exact value of the real part of refractive index is achieved. The discontinuity of the real part of refractive index at nearly 2.34 THz indicates that the proposed 3D metamaterial structure can no longer be considered as a homogenous medium. At the discontinuity point (nearly 2.34 THz), the real part of refractive index is $n = 2.73$ and the wavelength in medium is $\lambda \approx 47$ μm. The effective thickness of the proposed 3D metamaterial is $a = 50$ μm and $a/\lambda \approx 1$. Thus, we can explain this discontinuity as an upper limit of the effective medium theory. Effective electric permittivity and effective magnetic permeability of the second proposed 3D metamaterial are shown in Fig. 13.

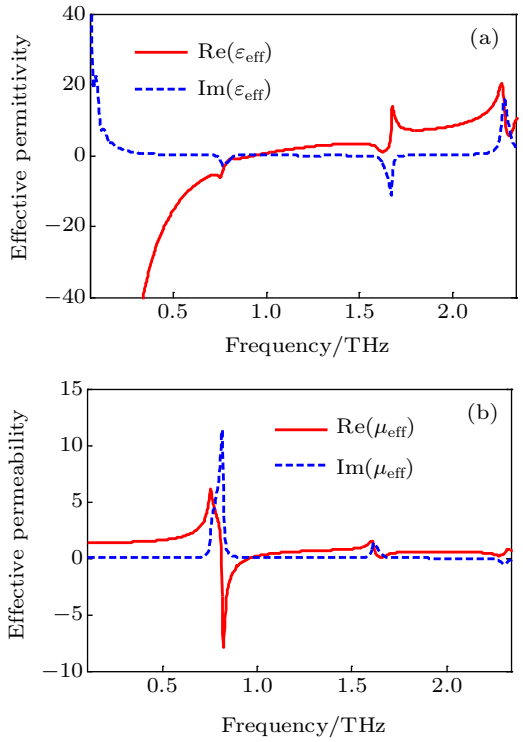


Fig. 13. (color online) Plots of (a) retrieved effective electric permittivity and (b) effective magnetic permeability versus frequency of the second 3D metamaterial structure.

6. Conclusion

In this paper, we numerically demonstrated two 3D metamaterial structures using an algorithm in which we employed the causality principle and Kramers–Kronig relations for accurately extracting effective parameters. After presenting the theory and formulation the algorithm is validated by retrieving the refractive index of a homogenous polymide cube. Using this algorithm, the proper branches of refractive index of proposed 3D metamaterials are selected. The proposed 3D metamaterial structures operate over the terahertz frequencies but with geometrical scalability, and this metamaterial could be designed to work in other frequency bands with negative refractive index.

References

[1] Smith D R, Padilla W J, Vier D C, Nemat-Nasser S C and Schultz S 2000 *Phys. Rev. Lett.* **84** 4184
[2] Schurig D, Mock J J, Justice B J, Cummer S A, Pendry J B, Starr A F and Smith D R 2006 *Science* **314** 977
[3] Pendry J B 2000 *Phys. Rev. Lett.* **85** 3966
[4] Fan Y N, Cheng Y Z, Nie Y, Wang X and Gong R Z 2013 *Chin. Phys. B* **22** 067801
[5] Cheng Y and Yang H 2010 *J. Appl. Phys.* **108** 034906
[6] Zhu B, Wang Z, Huang C, Feng Y, Zhao J and Jiang T 2010 *Prog. Electromagn. Res.* **101** 231
[7] Pendry J B, Holden A J, Stewart W J and Youngs I 1996 *Phys. Rev. Lett.* **76** 4773
[8] Pendry J B, Holden A J, Stewart W J and Robbins D J 1998 *J. Phys.: Condens. Matter* **10** 4785
[9] Pendry J B, Holden A J, Robins D J and Stewart W J 1999 *IEEE Trans. Microwave Theory Tech.* **47** 2075
[10] Baena J D, Marques R Medina F and Martel J 2004 *Phys. Rev. B* **69** 014402
[11] Wang D, Ran L, Chen H, Mu M, Kongand J A and Wu B I 2007 *Appl. Phys. Lett.* **90** 254103
[12] Chen H T, Padilla W, Cich M J, Azad A K, Averitt R D and Taylor A J 2009 *Nat. Photon.* **3** 148
[13] Tao H, Landy N I, Bingham C M, Zhang X, Averitt R D and Padilla W J 2008 *Opt. Express* **16** 7181
[14] Chen H T, O'Hara J F, Azad A K, Taylor A J, Averitt R D, Shrekenhamer D B and Padilla W J 2008 *Nat. Photon.* **2** 295
[15] He X J, Wang Y, Geng Z X, Wang J M and Gui T L 2011 *J. Magn. Magn. Mater.* **323** 2425
[16] Brener I, Burckel D B, Wendt J R, Ten Eyck G A, Ellis A R and Sinclair M B 2010 *SPIE Newsroom* 10.1117/2.1201007.003174
[17] Vignolini S, Yufa N A, Cunha P S, Guldin S, Rushkin I, Stefik M, Hur K, Wiesner U, Baumberg J J and Steiner U 2012 *Adv. Opt. Mater.* **24** 23
[18] Fan K, Strikwerda A C, Tao H, Zhang X and Averitt R D 2011 36*th International Conference on Infrared, Millimeter and Terahertz Waves,* October 2–7, 2011, Houston, TX, USA
[19] Valentine J, Zhang S, Zentgraf Th, Ulin-Avila E, Genov D A, Bartal G and Zhang X 2008 *Nature Lett.* **455** 376
[20] Gong B and Zhao X 2011 *Opt. Express* **19** 289
[21] Smith D R, Vier D C, Koschny Th and Soukoulis C M 2005 *Phys. Rev. E* **71** 036617
[22] Chen X D, Grzegorczyk T M, Wu B I, Pacheco J Jr and Kong J A 2004 *Phys. Rev. E* **70** 016608
[23] Varadan V and Ro R 2007 *IEEE Trans Microwave Theory Tech.* **55** 2224
[24] Szabó Z, Park G H, Hedge R and Li E P 2010 *IEEE Trans. Microwave Theory Tech.* **58** 2646
[25] Peiponen K E, Lucarini V, Vartiainen E M and Saarinen J J 2004 *Eur. Phys. J. B* **41** 61
[26] Nussenzveig H M 1972 *Causality and Dispersion Relations* (London and New York: Academic Press) pp. 15–28 and 43–45
[27] Fearn H 2006 *J. Mod. Opt.* **53** 2581
[28] Hou Z L, Kong L B, Jin H B, Cao M S, Li X and Qi X 2012 *Chin. Phys. Lett.* **29** 017701
[29] Wu B I, Wang W, Pacheco J, Chen X, Grzegorczyk T and Kong J A 2005 *Prog. Electromagn. Res.* **51** 295